SSC17-XII-01

The Active CryoCubeSat Project: Design and Status

Lucas Anderson, Charles Swenson
Center for Space Engineering
Utah State University
4130 Old Main Hill
Logan, Utah 84321
l.s.anderson@aggiemail.usu.edu

A. J. Mastropietro, Elham Maghsoudi, Simon Luong, Douglas Hofmann, Scott Roberts
Jet Propulsion Laboratory
California Institute of Technology
4800 Oak Grove Dr.
Pasadena, CA 91109
A.J.Mastropietro@jpl.nasa.gov

ABSTRACT

Under the NASA Small Spacecraft Technology Program, the Center for Space Engineering at Utah State University and NASA's Jet Propulsion Laboratory are jointly developing an active thermal control system to better enable cryogenic instrumentation on a CubeSat. The Active CryoCubeSat (ACCS) project is a two staged thermal architecture targeting 6U CubeSat platforms. The second stage consists of a miniature cryocooler for sub 100 K detector thermal management, while the first stage consists of a single phase Mechanically Pumped Fluid Loop that circulates a moderate temperature coolant between the cryocooler's cold plate heat exchanger (HX) and a radiator. As part of the investigation, two novel additive manufacturing techniques, Direct Metal Laser Sintering (DMLS) and Ultrasonic Additive Manufacturing (UAM), were also explored for the purpose of rapidly fabricating compact and lightweight liquid HX and radiator plates.

Instruments such as SABER on the NASA TIMED mission have used pulse tube cryocoolers to support multispectral scanning of the earth's atmospheric limb at infrared wavelengths. Such measurements require high radiometric sensitivity and can only be accomplished by cryogenically cooled detectors. The ACCS project hopes to enable similar CubeSat based missions such as the SABER-Lite miniature far-IR limb viewer. A summary and status of the project will be presented.

INTRODUCTION

The objective of the Active CryoCubeSat (ACCS) project, which is a NASA Small Spacecraft Technology Partnership between the Center for Space Engineering at Utah State University (USU) and the Jet Propulsion Laboratory (JPL), is to provide a ground based demonstration of an advanced thermal control system for a 6U CubeSat platform capable of high power management (>30W) and temperature regulation, while providing thermal accommodation of a cryogenic instrument. The thermal control system under development utilizes a two stage cooling architecture. The second stage consists of a miniature cryocooler to provide detector level cooling (>300 mW) in the cryogenic range of 75-100 K. The first stage is comprised of a small Mechanically Pumped Fluid Loop (MPFL)[1] that circulates a single phase, moderate temperature coolant between a liquid cold plate heat exchanger (HX) and an externally deployed radiator. As shown in Fig. 1, the entire heat load of the cryocooler (<15 W) along with the additional input power loads of the pump and any necessary controllers are transported by the first stage fluid loop to the external radiator for subsequent heat rejection. System interface temperatures can actively be maintained at ~35 ºC or less while overall power rejection greater than 55 W can potentially be achieved via active feedback and control of the MPFL's flow rate. The ACCS cryogenic thermal subsystem is designed to fit within a 1U volume, plus a thin deployable radiator, and targets standard, commercially available, 6U CubeSat platforms. However, larger small satellite platforms can be accommodated as the concept is entirely scalable. As part of this study, two novel additive manufacturing methods, Direct Metal Laser Sintering (DMLS) and Ultrasonic Additive Manufacturing (UAM), were explored as possible avenues to quickly build both miniature liquid HX and radiator plates while seeking to improve thermal performance and to potentially allow for the incorporation of the ACCS system directly into a small satellites' structure.

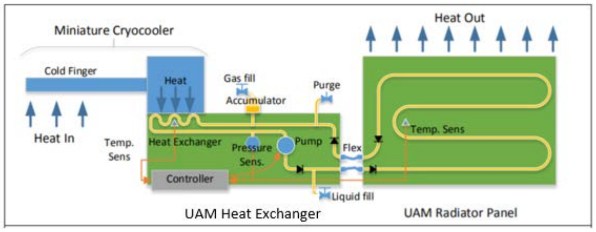

Figure 1: ACCS MPFL Thermal Accommodation of a Cryocooler

The primary objectives of the ACCS project are summarized in Table 1 along with the required performance benchmarks. Ultimately, the ACCS project will advance the development of CubeSat missions capable of cryogenic instrumentation for future NASA Science Mission Directorate programs[2].

Table 1: ACCS Project Objectives and Benchmarks

ACCS Project Objectives	
1)	Develop a miniature mechanically pumped fluid loop thermal control system for a CubeSat
2)	Develop advanced manufacturing techniques using Ultrasonic Additive Manufacturing (UAM) and Direct Metal Laser Sintering (DMLS) with aluminum to construct multifunctional structural-thermal components of a CubeSat
3)	Demonstrate thermal accommodation of a miniature cryocooler suitable for a cryogenic instrument
Required Performance	**Performance Goal**
MPFL	
Thermal Load: > 30 W Interface: 20-30°C Power: < 4 W Mass: < 2 kg Volume: < 1U Pointing: < .005°/s	Thermal Load: > 60 W Interface: 10-30°C Power: < 0.3 W Mass: < 0.5 kg Volume: < 0.3U Pointing: < .0005°/s
Additive Manufacturing	
10cm x 10cm HX Panel	10cm x 10cm HX Panel 20cm x 30cm Radiator
Cryocooler	
Temperature: < 100K Thermal Load: > 50 mW Power: < 15 W Mass: < 1 kg Volume: < 1U Stability: < .005°/s	Temperature: < 75K Thermal Load: > 250 mW Power: < 5 W Mass: < 0.2 kg Volume: < 0.3U Stability: < .0005°/s

SABER-LITE REFERENCE MISSION

The ACCS project was originally proposed as an advanced CubeSat reference mission inspired by NASA's Thermosphere, Ionosphere, Mesosphere, Energetics and Dynamics (TIMED) mission and the original USU Space Dynamics Lab developed Sounding of the Atmosphere in Broadband Emission Radiometry (SABER) instrument[3]. SABER measured the atmosphere using broadband limb-scanning infrared radiometry, covering the spectral range of 1.27 – 17 µm for mesosphere and thermosphere emissive trace species. The original SABER mission returns included the study of the fundamental process governing the chemistry, dynamics, and energetics of the upper atmosphere. The SABER instrument is cryogenically cooled and is still operating today onboard the TIMED spacecraft since its launch in 2001. The current TIMED spacecraft and SABER instrument are shown below in Fig. 2.

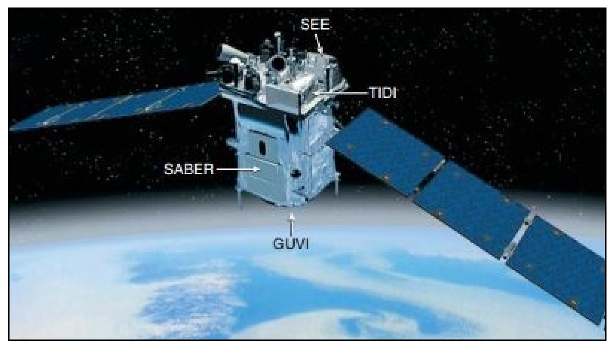

Figure 2: Original SABER Instrument on the TIMED Spacecraft[4]

The Center for Space Engineering (CSE) at USU has been developing a miniature SABER-Lite radiometer appropriate for CubeSat architectures and missions. The idealized reference mission includes the fully developed 1U ACCS thermal subsystem and the SABER-Lite instrument. The mission would seek to either replace, or complement the existing TIMED/SABER mission. Figure 3 shows the prototype SABER-Lite instrument "Tri-Clops" under development.

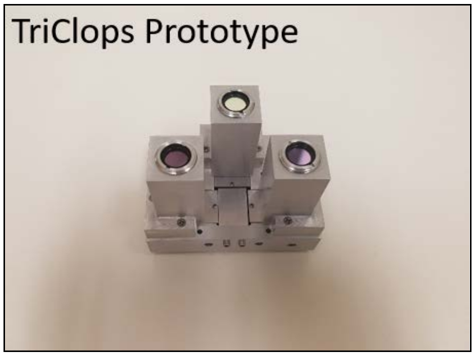

Figure 3: SABER-Lite "Tri-Clops" Radiometer Prototype

The reference mission considered would include a Blue Canyon Technologies bus customized to include the ACCS deployable radiator, the SABER-Lite radiometer, and the ACCS MPFL thermal control subsystem. The deployable radiator would feature a single, on orbit, flip down deployment off the nadir face of the bus chassis and a tracking beta drive. The SABER-Lite instrument would be limb viewing and sun shaded, while the solar panels would be zenith mounted. Figure 4 shows the high level conceptual configuration of the currently proposed ACCS/SABER-Lite mission.

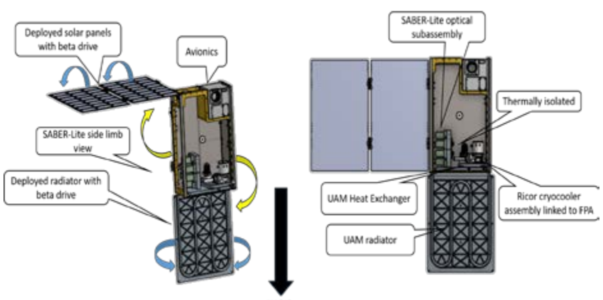

Figure 4: ACCS Accommodation of SABER-Lite Reference Mission

MICRO CRYOCOOLER SELECTION

Recent progress in cryocooler miniaturization has led to the development of both Stirling cycle & pulse tube cryocoolers that are appropriately sized for use within a CubeSat. Instrument concepts have been proposed for their use within small satellite missions. The ACCS project originally focused on the micro pulse tube cryocooler recently developed by Lockheed Martin (LM) to a TRL of 6[9]. The LM micro cryocooler features a low mass and a small volume form factor design with lower exported vibrations and a higher reliability (+100,000 hours) lifetime that makes it ideal for aerospace and CubeSat applications. LM originally planned to loan a micro cryocooler to the project team during the second year of the project; however, due to unforeseen scheduling complications the integration of the LM micro cryocooler into the ACCS ground based test bed has been delayed. Instead, the project team will integrate and test a miniature Ricor K508N Stirling cycle based cryocooler. The K508N features an integrated rotary system with an expanded lifetime of over 20,000 hours, and an increased ambient rejection temperature to power input ratio. Despite it being a greater source of vibration, the K508 was determined to be a suitable backup to the LM micro cryocooler owing in part to its successful implementation onboard the Curiosity rover[5]. Figure 5 shows both the LM Micro Cryocooler and the Ricor K508N cryocooler while Table 2 details the operating performance specifications of each unit. Fundamentally, the ACCS MPFL will serve as an ambient temperature control system for the miniature K508N cryocooler.

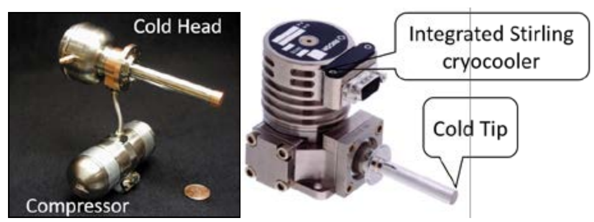

Figure 5: Lockheed Martin Micro & Ricor K508N Cryocoolers[6,7]

Table 2: Lockheed Martin Micro Cryocooler & Ricor K508N Cryocooler Performance Specifications[6-8]

Ricor K508N (Integrated Stirling Cycle)	
Cold Tip Temperature	77 K
Cold Tip Heat Load	~500 mW
Compressor Input Power	5-10 W
Ambient Reject Temperature Range	-40 ºC to +85 ºC
MTBF	+20,000 hr
Mass	454 gm
Form Factor	121x56.5x71 mm
LM Micro Cryocooler (Pulse Tube)	
Cold Tip Temperature	~90 K
Cold Tip Heat Load	~300 mW
Compressor Input Power	20 W
Ambient Reject Temperature Range	-30 ºC to -20 ºC
MTBF	+100,000 hr
Mass	311 gm
Form Factor	96.5x91.5x114 mm

WORKING FLUID SELECTION

The MPFL is the integral element of the ACCS system. Therefore, selecting an appropriate working fluid is an essential design aspect. While numerous fluids were considered, the decision was narrowed to five candidates. The parameters considered were:

- Density
- Viscosity
- Thermal Conductivity
- Specific Heat
- Liquid Vapor Pressure
- Safety
- Ease of use
- Cost & Availability

The physical properties over the temperature range of interest for each fluid as well as a decision summary matrix are provided in Figs. 6-10 and Table 3 respectively[10-13].

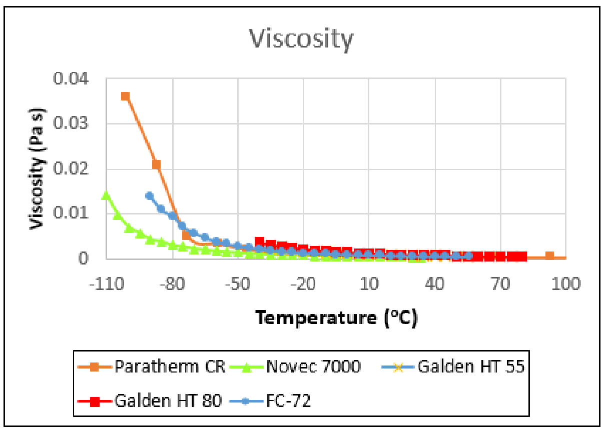

Figure 6: ACCS Working Fluid Comparison: Viscosity

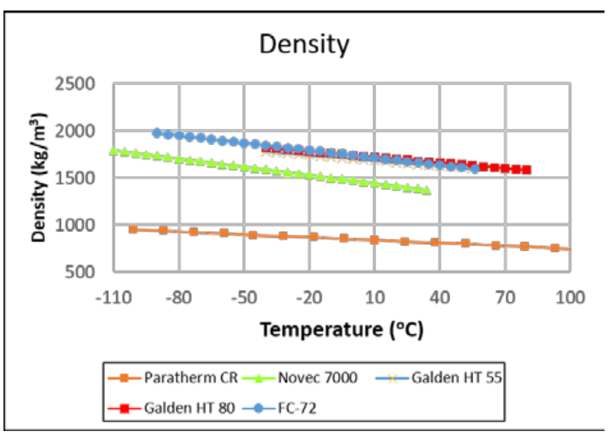

Figure 7: ACCS Working Fluid Comparison: Density

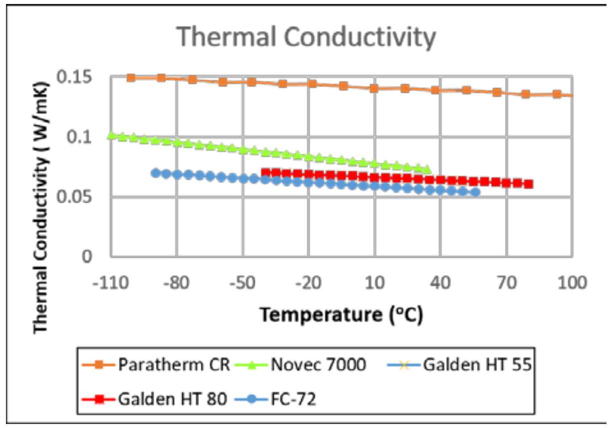

Figure 8: ACCS Working Fluid Comparison: Thermal Conductivity

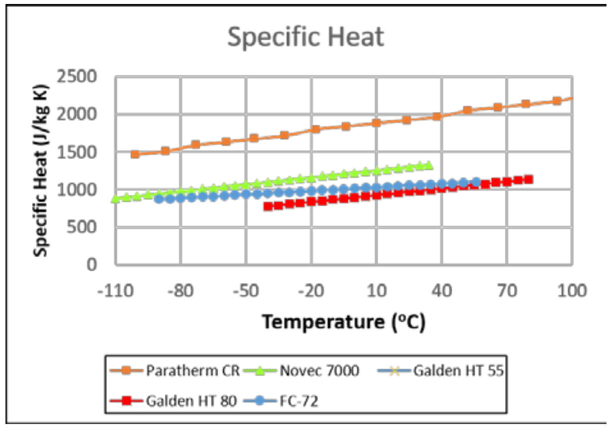

Figure 9: ACCS Working Fluid Comparison: Specific Heat

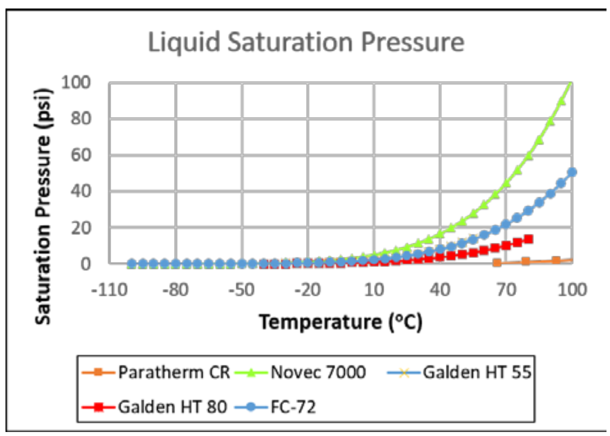

Figure 10: ACCS Working Fluid Comparison: Liquid Vapor Pressure

Table 3: Working Fluid Decision Matrix

Working Fluid Trade Study Decision Matrix						
Parameter	Thermal Conductivity	Specific Heat	Dynamic Viscosity	Density	Vapor Pressure	Pour Point
	W/mK	J/kgK	mPa sec	Kg/m^3	psi	℃
Effect	Thermal Transfer	Thermal Transfer	Decreases Pressure Drop	Reynolds #	Cavitation	Low Temp.
Fluid Req: -20 ℃	>0.1	>1000	<1.00	Approx. 1000	>0.34	<-100
Ranking						
	Best 1st	Good 2nd	Acceptable 3rd	OK 4th	Worst 5th	
Working Fluid Ranking						
Paratherm CR	1	1	2	5	1	-110
Novec 7000	2	2	1	4	5	-122
Galden HT 55	3	4	4	3	3	-115
Galden HT 80	3	4	5	2	2	-110
FC-72	5	3	3	1	4	-90
Hydrofluorocarbons: Novec 7000 & Silicone Oil: Paratherm CR @ -20 C						
Novec 7000	0.0797	1225.56	0.77	1530.2	1.129	-122
Paratherm CR	0.144	1787.17	1.35	871.43	NA	-110

The two fluids selected for testing with the ACCS system are Novec 7000, a low viscosity engineered hydrofluorocarbon and Paratherm CR, a silicone oil based thermal transfer fluid. Novec 7000 offers superior viscosity and therefore lower required pumping capacity. However, its reduced thermal performance requires higher flow rates for heat transfer and increased system pressure (>30 psi) to prevent boiling of the fluid at the elevated temperatures typically experienced by avionics. Paratherm CR is a superior heat transfer fluid and would not require additional pressurization to prevent two-phase flow. However, its viscosity and pumping performance are reduced at lower temperatures. Both fluids offer significant benefit to the ACCS project, and therefore the system will be characterized with the working fluid as another variable parameter.

MICRO PUMP SELECTION

A preliminary objective of the ACCS project was to perform a trade study on commercially available miniature pumps suitable for use within a CubeSat based MPFL. Eventually, the England manufacturer TCS Micropumps[14] was down selected for use within the ACCS MPFL - specifically, their line of low power, high flow centrifugal pumps, i.e. the M410 and M510 series. The parameters considered included:

- Large Potential Flow Rate
- Available Pressure Head
- Form Factor
- Mass
- Power
- Mechanical Noise (Vibration)
- Operational Lifetime
- Cost
- Efficiency
- Availability

Originally, the M410 series was selected due to meeting the requirements of pressure drop and flow rate while offering superior performance in terms of power, mass, size, and vibration. However, because of the requirement to run the ACCS system at a higher static pressure in order to prevent boiling and cavitation, it became apparent that there was an insufficient pressure rating on the internal seals within the pump assembly, thus the larger, more robust M510 was ultimately selected for incorporation into the vacuum test. The operating characteristics of the TCS M410 and M510 micro pumps are given below in Table 4.

Table 4. TCS Micropump Specifications[15, 16]

TCS M410 Operating Characteristics	
Maximum Flow Rate	up to 2600 mL/Min
Available Pressure	<5.5 psi
Power	<7 W
Form Factor	41 X 26 X 25 mm
Mass	32 grams
Mech. Noise	<3 dB
MTBF	>100,000hr
TCS M510 Operating Characteristics	
Maximum Flow Rate	up to 9000 mL/Min
Available Pressure	<10 psi
Power	<28 W
Form Factor	64 X 32 X 31 mm
Mass	100 grams
Mech. Noise	<15 dB
MTBF	>100,000hr

The M410 family of pump curves as a function of voltage input was developed using a custom designed pump characterization test setup capable of varying both the system impedance as well as the system operating temperature. Novec 7000 was used as the working fluid during the characterization effort. Figure 11 depicts a schematic of the experimental test setup. After the pump curves were measured, Excel and Matlab based tools were used to calculate the as designed ACCS system impedance as a function of flow rate. The calculation included both major and minor losses. Figure 12 shows the computed ACCS system impedance curve overlaid on the family of M410 pump curves in order to determine the potential operating point of the pump. The desired flow rate of 1200 mL/min and ~3psid of head requires a power input of ~7W. The same type of pump characterization testing is planned for the recently selected M510 pump. The M510 pump has much more capacity than the M410 at the expense of a higher power input; however, it's anticipated that it will be possible to achieve the project objectives with the M510 operating in a lower power consumption mode.

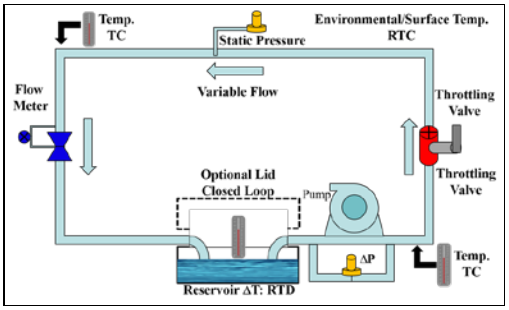

Figure 4: TCS M410 & M510 Pump Characterization Test Bed Schematic

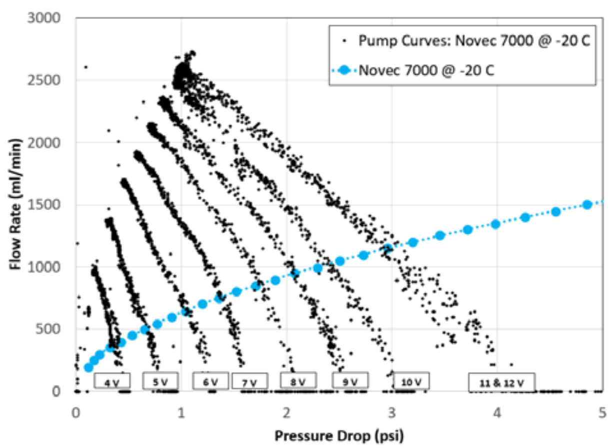

Figure 5: ACCS System Impedance Curve Overlaid on the Measured TCS M410 Pump Characterization Curves[15]

ADDITIVE MANUFACTURING OF LIQUID COLD PLATES AND THE CURRENT ACCS MECHANICAL DESIGN

As per the original ACCS proposal, aluminum based metallic additive manufacturing will be used to embed the various flow paths directly into the part of the CubeSat chassis that supports the cryocooler and pump mounts, as well as within a thin radiator panel. This serves the dual purpose of miniaturizing the system form factor and improving the thermal performance by circumventing traditional epoxy bonded or brazed tubing implementation. Furthermore, additive manufacturing should allow for a more rapid fabrication of a uniquely customized ACCS system, thereby enabling a better, more flexible design.

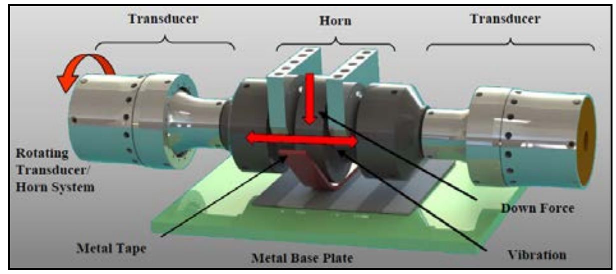

Figure 13: UAM Welding of Foil Tapes

Two novel additive manufacturing techniques were considered for the project – Direct Metal Laser Sintering (DMLS), and Ultrasonic Additive Manufacturing (UAM). There are some fundamental differences between these two technologies that are important to consider. DMLS is a high temperature, full melting fusion process of metallic powder that is currently limited to build size envelopes of 10"x10"x13" and print rates less than 1.8 cubic inches per hour. Aluminum parts can be fabricated from a casting alloy, $AlSi_{10}Mg$, as opposed to 6000 or 7000 series aluminum. The UAM process, on the other hand, as shown in Fig. 13 creates net-shape solid parts using low temperature solid state ultrasonic metal welding of foil sheets and tapes and traditional CNC contour milling. The high frequency back and forth scrubbing action of the ultrasonic weld head with its applied downward force breaks up the oxide layers between the constituents to be welded enabling cold state metallurgical bonding. Parts can be built as large as 6ft x 6ft x 3ft at a maximum print rate of 30 cubic inches per hour. 6000 and 7000 series aluminum parts as well as blended metallic parts such as Cu-Al, SS-Al are all possible. Despite these differences, DMLS is a much more established technology than UAM which is in its infancy.

Due to JPL's previous recent success with demonstrating the viability of using UAM to produce hermetically sealed HX structures[17], and owing in part to the fact that the industry leaders in UAM technology, Sheridan Solutions LLC and Fabrisonic LLC, have recently been awarded three NASA SBIRs to continue their development work of UAM aluminum based aerospace parts, UAM was selected as the primary method of fabrication for both the ACCS cold plate HX and radiator. In parallel, additional experiments comparing the hermetic and thermal performance of DMLS and UAM HX parts were also conducted at JPL[18-19]. Both additive manufacturing methods were found to be attractive over traditional based manufacturing methods.

Figures 14-16 detail the alternate cold plate HX designs considered for both the LM micro cryocooler and the Ricor K508N cryocooler, as well as the notional design for the deployable radiator. Each HX design incorporates the cryocooler compressor body, the cold finger assembly, the MPFL pump, and the controllers required to run the thermal subsystem. A pair of dale ohm heaters are also accommodated to maintain the minimum allowable pump and cryocooler assembly temperature during an instrument off case and also to help characterize additional heat rejection that could readily be achieved by the system. The radiator plate is mass optimized to be deployable.

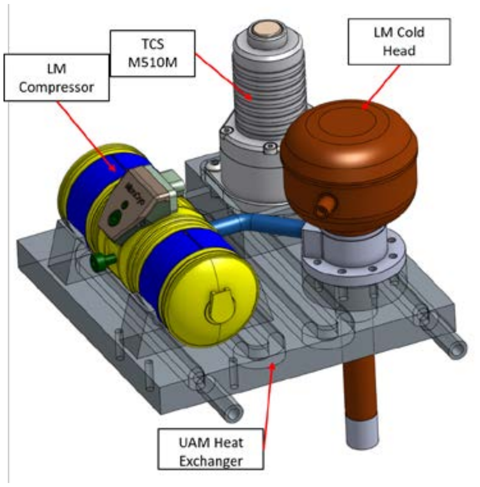

Figure 6: ACCS UAM HX Design for the LM Micro Cryocooler

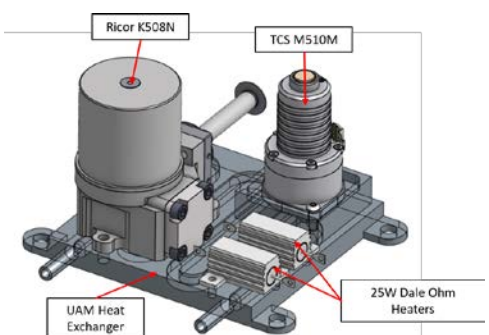

Figure 7: ACCS UAM HX Design for the Ricor K508N Cryocooler

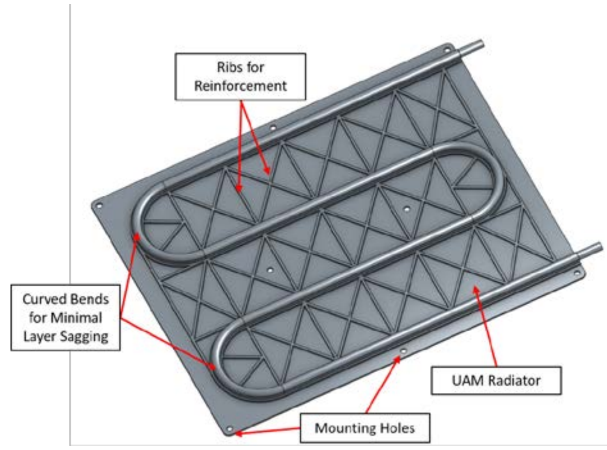

Figure 8: ACCS UAM Radiator Panel Design

Each cold plate design relies upon a combination of additive & subtractive manufacturing – an end mill is used to cut a U-shaped channel in a virgin billet of aluminum with as many passes as required for heat transfer, and then a roof consisting of multiple layers of aluminum foil sheet is ultrasonically consolidated over the channel. The part can then be light weighted anywhere outside the hermetically sealed cooling path as desired. The fabrication process is fully automatic with no tube bending or subsequent epoxy bonding or brazing required.

There were several important design considerations that had to be mechanically accommodated due to this additive approach to the hardware construction. Because the UAM weld head has a finite width, the roof over the channels is consolidated via multiple parallel passes. The most ideal weld head path avoids welding over milled channels that are oriented perpendicular to the direction of weld head travel. Due to the extreme downward force applied by the weld head roller, milled channels oriented perpendicular to the weld head path can experience sagging of the initial sheet layers into the profile of the milled channel. This perpendicular orientation of the channel permits an arc segment of the circular weld head roller to push slightly heated metal layers into the milled geometry. The realization of this tendency prompted design changes from sharp turning milled channels to channels having bends with a larger radius of curvature. This more forgiving geometry minimized the amount of sagging in these regions. Soft support material within the channels and a post UAM welding Hot Isostatic Press (HIP) process were also investigated to further decrease this sagging effect and were determined to be an excellent mitigation[20].

After several rigorous studies on UAM bond effectiveness over the coolant channels, another parameter which proved critical to consistent leak prevention was the minimum leak path dimension. For the purpose of this UAM study, this minimum dimension was maintained to be 0.100", and is measured from the point where the first layer weld meets the unsupported channel edge and extends radially outwards from that point. It is important to preserve this dimension in order to provide a sufficient region of fully supported UAM welding in order to ensure proper bonding of foil layers to prevent leaks and potential crack propagation.

Figures 17 and 18 show the as built UAM HX and radiator parts. They were subjected to bubble immersion testing to confirm no leaks were observed prior to part acceptance. The radiator panel was then black anodized to increase the surface emissivity in preparation for ground testing.

Other mechanical considerations which were taken into account when designing these parts include but are not limited to compacting the entire test bed design to fit into a very constrained vacuum chamber size, accommodating LN_2 shrouds positioned around the radiator, and allowing sufficient space for electrical signal feedthroughs and wrench access to enable fluid mechanical connections as well as fluid system charge and discharge.

Figure 17: UAM Radiator and HX Subjected to Bubble Immersion Leak Testing

Figure 18: As built UAM Radiator Panel with Black Anodize Surface Treatment

THERMAL ANALYSIS & MODELING

The ACCS is an active thermal fluid control system; therefore, an in depth understanding of the thermal performance and behavior of the system is required. To achieve this, a detailed analytical model/design tool was created and validated via Thermal Desktop®.

The model utilizes a piecewise or nodal approach beginning with a full environmental load study on the radiator for a reference orbit including: solar, albedo, and earthshine fluxes. Next, 2-D shape factors were used to model the heat rejected from the UAM embedded channels to the radiator surface. A constant surface temperature forced convection model was developed to describe the fluid thermal link between the cold radiator and the hot HX. Finally, 2D shape factors as well as simplified 1D conduction models were used to approximate the mounting surface temperature of the HX where the cryocooler, pump, and the various electronic boards are located. In addition, a full parasitic model was developed to calculate the expected thermal loads from the surrounding CubeSat to the cold finger of the cryocooler. A high level conceptual diagram of the MPFL thermal analysis, with nodes labeled, is given below in Fig. 19.

The thermal and hydraulic design is a trade-off between the heat rejection capability of the system and the pressure drop within the system. As the average flow velocity increases, turbulent characteristics and heat rejection become stronger; however, pressure drop also increases. Therefore, the goal of this thermal design is to compromise between reasonable HX and radiator channel lengths, as well as channel size, while maintaining a moderate pumping head requirement for the system. For these reasons, the current MPFL design targets Reynolds numbers of greater than 4500 for Paratherm CR, and ~8500 for Novec 7000. In theory, the ACCS system can toggle between laminar and turbulent flow regimes by throttling the pump speed in order to maintain a steady loop operating temperature despite fluctuations in equipment dissipation or environmental loads. Table 5 provides a summary of the equations used in the analysis.

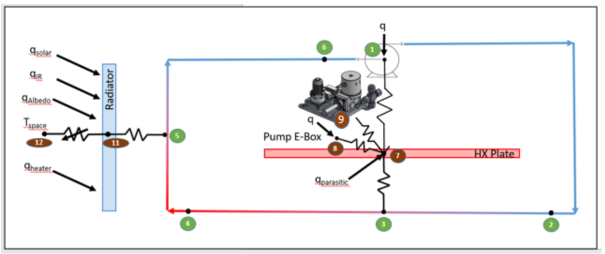

Figure 19. Simple Nodalized Model of the MPFL System.

Table 5: ACCS Analysis Working Equations[21-25]

Nusselt Number	Equation
Laminar Flow Re<2300	$Nu_D = 3.66$
Transitional Regime 3000<Re<5×10[6]	$Nu_D = \dfrac{\left(\frac{f}{8}\right)(\mathrm{Re}_D - 1000)\mathrm{Pr}}{1+12.7\left(\frac{f}{8}\right)\left(\mathrm{Pr}^{\frac{2}{3}} - 1\right)}$
Turbulent Flow Re>10000	$Nu_D = 0.023(\mathrm{Re})^{4/5}\,\mathrm{Pr}^n$
Friction factor 2300 < Re < 5×10[6]	$f = 0.79.Ln(\mathrm{Re} - 1.64)^{-2}$
Pressure Head	
Modified Bernoulli	$\Delta P = \rho g\left[\left(\dfrac{V_2^2 - V_1^2}{2g}\right) + (z_2 - z_1)\sum \dfrac{fL}{D_h}\dfrac{V^2}{2g} + \sum K \dfrac{V^2}{2g}\right]$
Modified Bernoulli with major + minor losses + 2k method	$K = \dfrac{K_1}{\mathrm{Re}} + K_\infty\left(1 + \dfrac{D}{2}\right)$ $\Delta P = \rho \dfrac{V^2}{2}\left[\left(\dfrac{f.l}{D}\right) + \sum N.K\right]$

Figures 20 and 21 detail how the pressure drop and total heat rejection of the ACCS system varies with temperature for Novec 7000 and Paratherm CR, while Figs. 22 and 23 demonstrate the same variations with respect to Reynolds number. It should be noted, that a 3 K temperature gradient between the mounting surface interface and the average fluid temperature within the embedded HX channels was assumed as a design goal. Table 6 details the scope of a few of the ACCS system design points.

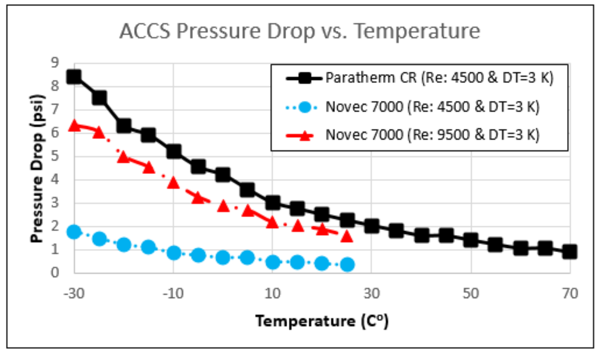

Figure 20: ACCS System Pressure Drop vs. Temperature for Paratherm CR & Novec 7000

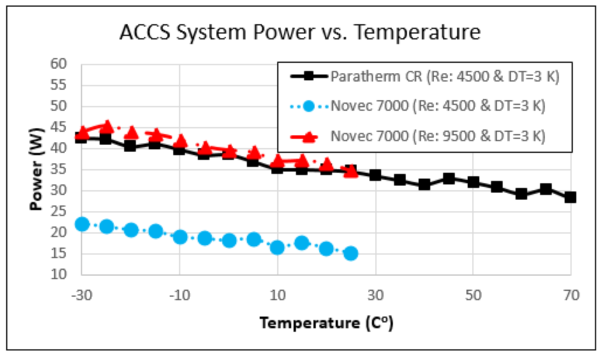

Figure 21: ACCS System Heat Rejection vs. Temperature for Paratherm CR & Novec 7000

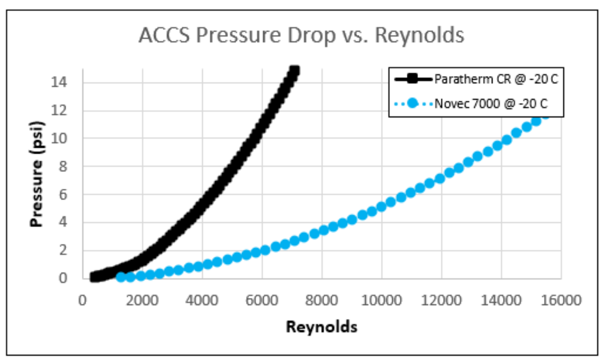

Figure 92: ACCS System Pressure Drop vs. Reynolds Number for Paratherm CR & Novec 7000

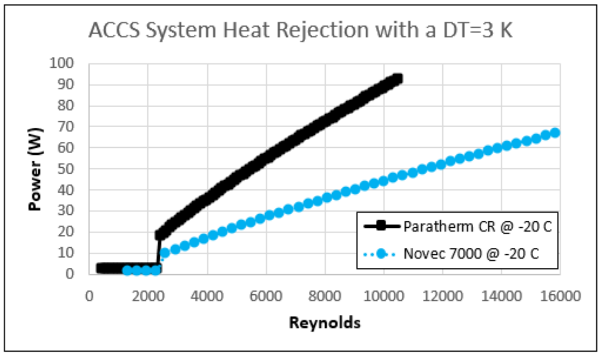

Figure 23: ACCS System Heat Rejection vs. Reynolds for Paratherm CR & Novec 7000

Table 6: ACCS Specifications

ACCS Design Parameters: Paratherm CR	
Total Internal Dissipation	30 W
Radiator Surface Temperature	-20.4 ºC
HX I/F Temperature	-17 ºC
Total I/F Length	55 cm (HX) & 122 cm (Rad.)
Flow Rate	~2.2 L/min (Nominal)
Reynolds Number	~4,500 (Nominal)
$m_{dot}Cp$	~57 W/K (Nominal) @ -20 ºC
I/F Conductance	~25 W/mK @ -20 ºC
Convective Coefficient	~1200 W/m^{2}K @ -20 ºC
System Pressure Drop	<6.5 psid
ACCS Design Parameters: Novec 7000	
Total Internal Dissipation	30 W
Radiator Surface Temperature	-20.4 ºC
HX I/F Temperature	-16.6 ºC
Total I/F Length	55 cm (HX) & 122 cm (Rad.)
Flow Rate	~1.4 L/min (Nominal)
Reynolds Number	~9,000
$m_{dot}Cp$	~44 W/K (Nominal) @ -20 ºC
I/F Conductance	~27 W/mK @ -20 ºC
Convective Coefficient	~1200 W/m^{2}K @ -20 ºC
System Pressure Drop	<4.5 psid

Ultimately, the analytical model developed for the ACCS system serves as an iterative design tool for the project and as a method of predicting the performance and behavior of the ACCS system.

Thermal Desktop® was used to validate the reference orbit environmental loads for the analytical system model and it was used to provide a more thorough understanding of the temperature gradients within the HX and radiator. Figure 24 displays the resulting temperature contour plot of the HX assuming a constant inlet temperature and constant heat dissipations for the pump and the LM micro cryocooler. Figure 25 shows the resulting temperature contour plot for the radiator model which was used to determine the optimal number of channel passes. The overall fin efficiency formulation was simplified to calculate the general radiator efficiency as:

$$\eta = \frac{T_{av}^{\ 4}}{T_{inlet}^{\ 4}} \qquad 1)$$

where T_{av} is the area weighted average surface temperature of the radiator, in degrees Kelvin, and T_{inlet} is the fluid inlet temperature, also in degrees Kelvin. As the number of passes was increased beyond four, no significant change in efficiency was observed. Thus, a total of four passes was recommended for the radiator design yielding an efficiency of 97%.

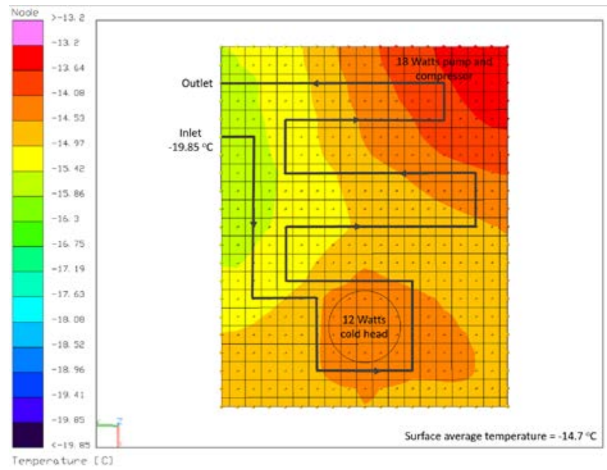

Figure 24: Thermal Desktop® Temperature Contour Plot of the ACCS HX for LM Micro Cryocooler

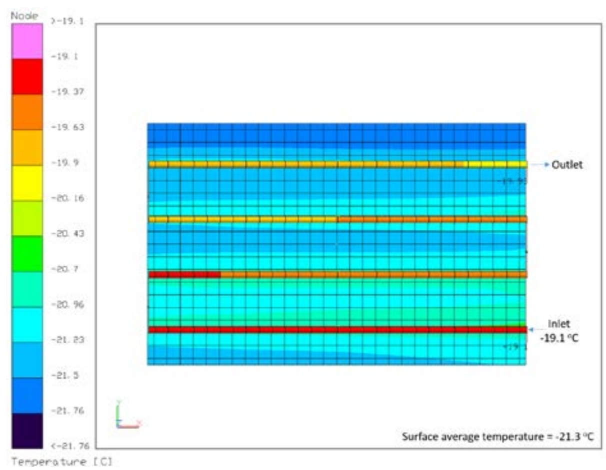

Figure 10: Thermal Desktop® Temperature Contour Plot of the ACCS Radiator Panel

ACCS CHARACTERIZATION TEST

The objective of the current project is to demonstrate the ACCS system in a relevant laboratory based environment and to raise the overall TRL to 4. To accomplish this a characterization test setup and procedure has been developed. The test setup consists of a vacuum chamber, LN_2 shrouding and MLI blanketing to maintain the radiation sink temperature, and strategically placed heaters to simulate excess dissipation or fluctuations in either the orbital environment or parasitic heat load absorbed by the cryocooler cold finger. The UAM HX and UAM radiator are connected to one another via tubing and the entire assembly is thermally isolated. A National Instruments data logger along with a variety of sensors are used to monitor the performance of the ACCS system. Table 7 lists the sensors and their function while Fig. 26 is a diagram of the ACCS characterization test setup.

Table 7: Sensor & Data Logging Components

Sensor list **MPFL performance**	Function
Type T Thermocouples	Surface + emersion temp.
Thermal IR Camera	Provide an analog temp. comparison
Delta P Transducers	Log the systems total differential pressure drop + static pressure level
Flow Rate: • Venturi • Turbine	Monitor the systems flow rate
Power monitoring	
Cryocooler	Monitor the power profile performance of the cryocooler
Pump power	Monitor the 3-phase power profile of the pump as well as the RPM's via back EMF
Heat Exchanger heater	Simulates system power loads
Radiator Heater	Simulates environmental loading
Cold Tip Heater	Simulates cryogenic instrument loading

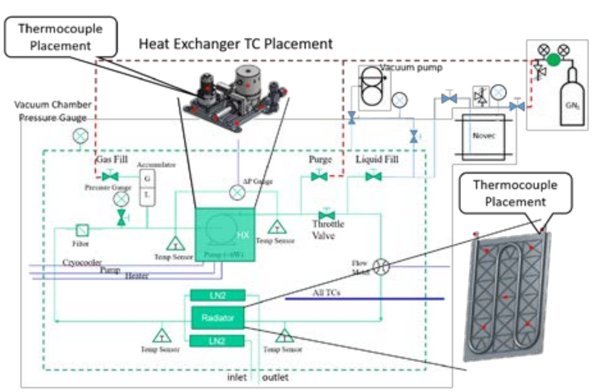

Figure 26: Schematic of the ACCS Characterization Test Setup

The test procedure for the ACCS characterization begins with purging and filling the MPFL loop. Next, the pump is turned on as well as the cryocooler. The system is allowed to cool via radiation through the integrated LN2 shrouds surrounding the radiator panel. Once the desired thermal equilibrium has been reached heaters on the HX may be turned on to vary the system power load. The pump will be throttled through laminar and turbulent flow regimes to maintain the targeted interface temperatures. It should be noted that both the LM micro cryocooler and the Ricor K508N are self-contained in terms of their control and feedback. Therefore, only the HX heaters, cold finger heater, and pump flow rate will be varied to bound the system performance.

ACCS FUTURE WORK

The near term objectives of the Active CryoCubeSat project are to finalize the characterization test setup and procedure and to run the ACCS active thermal control system to verify its power rejection capability over a variety of conditions and measure its ability to maintain near constant interface temperatures with small variations in power. In addition, if time permits, the team plans to further explore the LM micro cryocooler along with additional working fluids. In parallel, the CSE team will continue its development of SABER-Lite and hopes to be in a better position to win proposals enabling either a balloon based mission or a real spaceflight CubeSat mission.

CONCLUSIONS

The Active CryoCubeSat team has successfully developed a series of design concepts, and thermal fluid modelling tools, allowing for the theoretical characterization of a miniature (1U) thermal control subsystem appropriate for CubeSat's platforms and missions. This combined with the CSE team's work on the SABER-Lite radiometer, has allowed for the rapid design iteration of a SABER-Lite reference mission. In addition, a rigorous study of the current industry standard has allowed a system design comprised of largely off the shelf commercially available components. UAM based heat exchangers and radiator prototypes have been designed and manufactured, and a relevant ground based test architecture has been developed for the purpose of characterizing the ACCS system. A miniature cryocooler has been integrated within the system to allow for a report on the system's ability to enable cryogenic instrumentation on a Small Satellite. Ultimately, the ACCS team has made tremendous progress and looks forward to reporting on the system performance pending the completion of the ground testing.

ACKNOWLEDGMENTS

Part of the development described was performed at the Jet Propulsion Laboratory, California Institute of Technology, under a contract with the National Aeronautics and Space Administration. The project team would like to thank NASA's Space Technology Mission Directorate SBIR Program Management Office and its Small Spacecraft Technology Program Management Office as well as USU's and JPL's Internal R&TD Program Management Office for enabling this work. Specifically, the authors would like to acknowledge the following individuals for their contributions and invaluable support: James Cockrell (NASA Ames Research Center), Jeffrey Olson (Lockheed Martin), Mark Norfolk (Fabrisonic LLC), John Sheridan (Sheridan Solutions LLC), Alan Marchant (USU CSE), Scott Jensen (Tempus Global Data), Gregory Davis (JPL), Timothy O'Donnell (JPL), Nickolas Emis (JPL), Eric Sunada (JPL), Gordon Cucullu (JPL), Fred Hadaegh (JPL), Saverio D'Agostino (JPL), Michael Pauken (JPL), Abdullah Aljabri (JPL), Bryan Mcenerney (JPL), Raymond Higuera (JPL), Brian Carroll (JPL), Sandro Torres (JPL), Bradley Kinter (JPL), Stefano Cappucci (JPL), Ben Furst (JPL), Joel Steinkraus (JPL), and Ian McKinley (JPL). In addition, the ACCS project would not exist without the dedicated undergraduate research team of USU's CSE: Russell Babb, Dana Sorensen, Patrick Mortola, Colton Lundstrom, Caleb Young, and Nathon Tipton.

ACRONYMS

- ACCS Active CryoCubeSat
- CNC Computer Numerical Control
- CSE Center for Space Engineering
- DAQ Data Acquisition
- DMLS Direct Metal Laser Sintering
- EMF Electromotive Force
- HIP Hot Isostatic Press
- HX Heat Exchanger
- I/F Interface
- IR Infrared
- JPL Jet Propulsion Laboratory
- LEO Low Earth Orbit
- LM Lockheed Martin
- MLI Multi-Layer-Insulation
- MPFL Mechanically Pumped Fluid Loop
- MTBF Mean Time Between Failures
- NASA National Aeronautics and Space Administration
- R&TD Research and Technology Development
- SABER Sounding of the Atmosphere in Broadband Emission Radiometry
- SBIR Small Business Innovative Research
- TIMED Thermosphere, Ionosphere, Mesosphere, Energetics, and Dynamics
- TRL Technical Readiness Level
- UAM Ultrasonic Additive Manufacturing
- USU Utah State University

NOMENCLATURE

c_p = specific heat, J/(kg-K)
D = tube diameter, m
f = friction factor
g = acceleration, m/s^2
h = convective heat transfer coefficient, W/(m^2.K)
k_f = fluid thermal conductivity, W/(m.K)
K = fittings and bends loss coefficient
l = tubing length, m
m_{dot} = mass flow rate, kg/s
n = 0.4 heated flow
N = number of fittings and bends
Nu_D = Nusselt number based on the tube diameter
P = pressure, Pa
Pr = nondimensional Prandtl number
Re_D = Reynolds number based on the tube diameter
T = temperature, ºC
T_{av} = average surface temperature, K
T_{inlet} = inlet fluid temperature, K
V = average velocity, m/s

Greek symbols

ρ = density, kg/m^3
ΔP = pressure drop, Pa
η = radiator efficiency

REFERENCES

[1] Mastropietro, A. J., Bhandari, Pradeep, Birur, Gajanana, et. al., "Summary and Status of 5 Mechanical Pumped Fluid Loop (MPFL) Projects Currently in Process at the Jet Propulsion Laboratory (JPL) for the Planned Europa Mission, Mars 2020, Ecosystem Spaceborne Thermal Radiometer Experiment on Space Station (ECOSTRESS), Orbiting Carbon Observatory (OCO-3), and Cold Atom Lab (CAL)," Thermal and Fluids Analysis Workshop (TFAWS), Mountain View, CA, August 2016.

[2] NASA, Active CryoCubeSat [Online] June 2017, https://ntrs.nasa.gov/archive/nasa/casi.ntrs.nasa.gov/20160007914.pdf

[3] David Y. Kusnierkiewicz, "An Overview of the TIMED Spacecraft" [Online] September 2016, http://www.jhuapl.edu/techdigest/TD/td2402/Kusnierkiewicz1.pdf

[4] Chunmei Kang, "TIMED: Mission Overview and Satellite Sampling Discussion" [Online] September 2016, http://ccar.colorado.edu/asen5050/projects/projects_2004/kang/

[5] D. L. Johnson, M. J. Lysek and J.M. Morookian, 2014, "The Ricor K508 cryocooler operational experience on Mars", AIP Conference Proceedings, Volume 1573, 1792-1799

[6] Lockheed Martin Advanced Technology Center, "Satellite Cooling System Breakthrough Developed by Lockheed Martin Space Systems" [Online] September 2016, http://www.lockheedmartin.com/content/dam/lockheed/data/space/photo/pressrelease/Microcryocooler.jpg

[7] Integral Rotary Integral Stirling 1/2W Micro Cooler K508N [Online] June 2017, http://www.ricor.com/products/integral-rotary/k508n/

[8] Itai Regev, Ilan Nachman, Dorit Livni, Sergey Riabzev, Avishai Filis, Victor Segal, "RICOR Development of the Next Generation of Highly Reliable Rotary Cryocoolers," Proc. SPIE 9821, Tri-Technology Device Refrigeration (TTDR), 982109 May 17, 2016.

[9] I. M. McKinley, D. L. Johnson and J. I. Rodriguez, "Characterization Testing of Lockheed Martin Standard Micro Pulse Tube Cryocooler," Cryocoolers 19, ICC Press, Boulder, CO 2016.

[10] Paratherm CR Heat Transfer Fluid, [Online] June 2017,

http://www.paratherm.com/heat-transfer-fluids/paratherm-cr-heat-transfer-fluid/

[11] 3M™ Novec™ 7000 Engineered Fluid [Online] June 2017,

http://multimedia.3m.com/mws/media/121372O/3m-novec-7000-engineered-fluid-tds.pdf

[12] Galden HT PFPE Heat Transfer Fluid [Online] June 2017, http://www.behlke.com/pdf/datasheets/galden_ht135.pdf

[13] 3M Fluorinert™ Electronic Liquid FC-72 [Online] June 2017,

http://multimedia.3m.com/mws/media/64892O/fluorinert-electronic-liquid-fc-72.pdf

[14] TCS Micropumps-High Performance Miniature Pumps [Online] June 2017,

http://www.micropumps.co.uk/

[15] M410 Series – Data Sheet [Online] June 2017, http://www.micropumps.co.uk/DATA/pdf/DS26%20-%20M410%20Data%20Sheet%20REV%201%20SMALL.pdf

[16] M500 Series – Data Sheet [Online] June 2017, http://www.micropumps.co.uk/DATA/pdf/DS05%20-%20M500%20Data%20Sheet%20REV%206%20small.pdf

[17] Mastropietro, A. J., Pauken, Michael, Hofmann, Douglas, D'Agostino, Saverio, "Ultrasonic Additive Manufacturing (UAM) of Heat Rejection System (HRS) Heat Exchangers," Innovative Spontaneous Concept R&TD, Annual Report to JPL's R&TD Program Office, 2014.

[18] Sunada, Eric, and Rodriguez, Jose, "JPL Advanced Thermal Control Technology Roadmap," Spacecraft Thermal Control Workshop, El Segundo, CA 2017.

[19] Maghsoudi, Elham, Mastropietro, A. J., Roberts, Scott, and Kinter, Bradley, "Experimental Thermal Performance Comparison of 3D Printed Aluminum Heat Exchangers vs Traditionally Manufactured Heat Exchangers," Spacecraft Thermal Control Workshop (STCW), El Segundo, CA, March 2017.

[20] Mastropietro, A. J., Roberts Scott, Hofmann Douglas, Maghsoudi, Elham, and Luong, Simon, "NASA Development of Complex Heat Exchangers Leveraging Additive Manufacturing," Propulsion Safety and Sustainment Conference, Phoenix, AZ, May 2017.

[21] Incropera, F.P., and DeWitt, D.P., "Introduction to Heat Transfer," 3rd ed., John Wiley & Sons, 1996.

[22] Howell, J.R., Menguc, M.P., Siegel, R., "Thermal Radiation Heat Transfer," 6th ed., CRC Press, 2016.

[23] Janna, W.S., "Design of Fluid Thermal Systems," 2nd ed., PWS Publishing Company, 1998.

[24] Gilmore, D.G., "Spacecraft Thermal Control Handbook: Volume 1: Fundamental Technologies," 2nd ed., The Aerospace Press, 2002.

[25] Sadik Kakac, Ramesh K. Shah, and Win Aung, "Handbook of Single-Phase Convective Heat Transfer," 1st Edition, John Wiley, 1987.